Published in final edited form as:
Biochim Biophys Acta. 2011 December ; 1808(12): 3016–3021. doi:10.1016/j.bbamem.2011.08.004.

Differential expression of human riboflavin transporters -1, -2, & -3 in polarized epithelia: a key role for hRFT-2 in intestinal riboflavin uptake

Veedamali S. Subramanian[1,2], **Sandeep B. Subramanya**[1,2], **Laramie Rapp**[3], **Jonathan S. Marchant**[3], **Thomas Y. Ma**[4], and **Hamid M. Said**[1,2]

[1]Departments of Medicine and Physiology/Biophysics, University of California Medical School, Irvine, CA 92697

[2]VAMC, Long Beach, CA 90822

[3]Department of Pharmacology, University of Minnesota Medical School, MN 55455

[4]Department of Internal Medicine, University of New Mexico, NM 87131

Abstract

Transport of riboflavin (RF) across both the brush border membrane (BBM) and basolateral membrane (BLM) of the polarized enterocyte occurs via specific carrier-mediated mechanisms. Although, three human riboflavin transporters (hRFTs), i. e., hRFT-1, hRFT-2 and hRFT-3 are expressed in the intestine, little is known about the cell surface domain(s) at which these specific hRFTs are expressed. Here, we used live cell confocal imaging of intestinal epithelial Caco-2 and renal MDCK cells to show that the hRFT-1 is mainly expressed at the BLM, hRFT-2 is exclusively expressed at the apical membrane, while hRFT-3 is mostly localized inside intracellular vesicular structures (with some expression at the BLM). Further the level of hRFT-2 mRNA expression in Caco-2 cells and in native human intestine is significantly higher than that of hRFT-1 and -3; hRFT-2 was also more efficient in transporting ^{3}H-RF than hRFT-1 and -3. These findings implied an important role for hRFT-2 in intestinal RF uptake, a conclusion that was further supported by findings of hRFT-2 gene-specific siRNA knockdown investigation. These results show that members of the hRFT family are differentially expressed in polarized epithelia, and that the apically expressed hRFT-2 plays a key role in intestinal RF accumulation.

Keywords

Transport; intestine; epithelia; polarity; targeting

1. Introduction

Riboflavin (RF; vitamin B2) is an essential micronutrient for normal cellular growth and function. In its coenzyme forms [riboflavin-5-phosphate and flavin adenosine dinucleotide], the vitamin plays key metabolic roles in biological oxidation-reduction reactions involving

Address all correspondence to H. M. Said, VA Medical Center-151, Long Beach, CA 90822, Tel: (562) 826-5811, Fax: (562) 826-5675, hmsaid@uci.edu.

lipid, carbohydrate and amino acid metabolism, as well as in cellular metabolism of other water-soluble vitamins [1]. RF deficiency and sub-optimal RF levels occur in conditions like chronic alcoholism, diabetes mellitus, and inflammatory bowel diseases as well as in the elderly [2–6]. Deficiency of RF leads to a variety of clinical abnormalities that include neurological disorders, anemia, growth retardation, and skin abnormalities [1, 7] as well as an increased susceptibility to cancer [8].

Mammals, including humans, have lost the capability for *de novo* synthesis of RF and obtain the vitamin from exogenous sources via intestinal absorption. The human intestine encounters RF from two sources: a dietary source (processed and absorbed in the small intestine), and a bacterial source from the normal large intestine microflora (absorbed in the large intestine) [9–13]. The mechanism of absorption of free RF has been studied using a variety of human and animal intestinal preparations [reviewed in 14]. Collectively, these studies have shown that absorption of RF in the small and large intestine is mediated by an efficient and specific, carrier-mediated mechanism. Since absorption of a nutrient across polarized intestinal epithelial cells represents movement across two functionally and structurally distinct membrane domains [brush border membrane (BBM) and basolateral membrane (BLM) domains], studies have also examined the mechanism(s) of RF transport across the individual membrane domain using purified membrane vesicles with results showing a specific carrier-mediated mechanism existing at each membrane domain [15–18]. Recently, molecular identity of the RFT systems that operate in human tissues has been defined. Three human riboflavin transporters, hRFT-1, hRFT-2 and hRFT-3 have been cloned [19–21] and all were shown to be expressed in the human intestine [19]. hRFT-1 and -3 share 87 percent identity at amino acid levels, whereas hRFT-2 shares 43 and 44 percent identity with hRFT-1 and -3, respectively [19]. Little, however, is known about the membrane domain(s) of the polarized enterocyte at which these different transporters are localized. Addressing this issue is crucial for understanding the details of the intestinal RF absorption process. Here, we investigated this issue using live cell confocal imaging in confluent monolayers of a polarized intestinal epithelial Caco-2 and renal epithelial MDCK cell types. Our findings demonstrate that the hRFT-1 is mainly expressed at the BLM, while expression of the hRFT-3 occurs predominantly in intracellular vesicles (with some being at the BLM). Expression of the hRFT-2, on the other hand, occurs exclusively at the apical membrane domain [21, 22]. These findings together with functional data involving both over-expression and selective knockdown with gene-specific siRNA, suggest a predominant role for the hRFT-2 in intestinal RF absorption.

2. Materials and Methods

2.1. Materials

GFP-C3 and DsRed-C1 fluorescent protein vectors were from Clontech (Palo Alto, CA). LAMP1-RFP was obtained from Addgene Inc (Cambridge, MA). Caco-2, HuTu-80 and MDCK cells were from ATCC (Manassas, VA). ^{3}H-RF (specific activity ~12.3Ci/mmol) was from Moravek Biochemicals (Brea, CA). DNA oligonucleotides primers (Table 1) were synthesized by Sigma Genosys (Woodlands, TX). hRFT-2 gene specific siRNA was from Invitrogen (Carlsbad, CA; Table 1).

2.2. Generation of fluorescent protein fusion constructs

The full-length GFP-hRFT1, GFP-hRFT2, DsRed-hRFT2 and GFP-hRFT3 were generated by PCR amplification using hRFT-1, -2, and -3 gene specific primer combinations (Table 1), PCR amplification kit (Clontech, CA) and PCR conditions as described previously [22–24]. The amplified PCR products for hRFT-1 and -3 and GFP-C3 vector were digested with *Hind III* and *Sac II*. The PCR product for hRFT-2, DsRed-C1 and GFP-C3 vectors were digested

with *XhoI*/*SalI* and *BamHI*. The digested products were ligated separately for each construct using rapid DNA ligation kit (Roche Diagnostics, Indianoplis, IN) to generate in-frame fusion construct with GFP-C3 or DsRed-C1 fused to NH_2- terminus of each full-length construct. The generated fusion constructs were all verified by sequencing (Laragen, Los Angeles, CA).

2.3. Cell culture and transient transfection

Caco-2, HuTu-80 and MDCK cells were maintained in minimal essential medium [(MEM) ATCC, Manassas, VA]. MEM was supplemented with fetal bovine serum, glutamine, $NaHCO_3$ and antibiotics as described before [22–24]. Cells were grown on sterile glass-bottomed poly-D-lysine coated petri-dishes (MatTek, MA) or on 12 well plates (Corning, NY) and transfected with GFP, GFP-hRFT1, GFP-hRFT2, DsRed-hRFT2 and GFP-hRFT3 at 95% of confluency with 2–4 μg of plasmid DNA using Lipofectamine 2000 (Invitrogen, CA) [22, 25]. After 24–48hrs of transient transfection, cells were imaged on petri-dishes or used for ^{3}H-RF uptake as described below.

2.4. Confocal imaging of fluorescent protein fusion constructs in live cells

Confluent cell monolayer was imaged using a Nikon C-1 confocal microscope. Green fluorescent protein (GFP) was excited with 488nm line from an argon ion laser and emitted fluorescence was monitored with a 515±30nm short pass filter (GFP), Red fluorescent protein (DsRed) was excited with the 543-nm line from an HeNe ion laser and emitted fluorescence was monitored with a 570±50nm long pass filter. Images were captured using Nikon C-1 software (Nikon Instruments Inc, NY) [22, 25].

2.5. siRNA treatment

hRFT-2 gene-specific siRNA was obtained from Invitrogen (Carlsbad, CA) with a sequence as listed in Table 1. Caco-2 cells pretreated with (60 nM) hRFT-2 siRNA or control siRNA (scrambled siRNA) for 48hrs and were used for ^{3}H-RF uptake and for RNA isolation to perform real-time PCR analysis as described below.

2.6. ^{3}H-RF uptake assay

^{3}H-RF uptake assays were performed on GFP-hRFT1, GFP-hRFT2 and GFP-hRFT3 transiently expressing HuTu-80 cells, or hRFT-2 gene-specific siRNA pretreated Caco-2 cells in Krebs-Ringer buffer (pH 7.4) containing ^{3}H-RF (0.025 μM) as described previously [22, 25]. Protein content of the cell digest was determined in parallel wells using protein assay kit (Bio-Rad, CA).

2.7. Real-time PCR analysis

Native human small intestinal RNA [pooled from 5 individuals (Clontech, CA)] or RNA isolated from Caco-2 cells was used for real-time PCR analysis. cDNA was synthesized from RNA using a reverse transcriptase kit (Invitrogen, CA) and real-time PCR was performed utilizing hRFT-1, -2, -3 and β-actin selective primers as described before [22, 26, 27].

2.8. Statistical analysis

Uptake data represent the result of three separate experiments and are expressed as mean ± SE in fmol/mg protein/unit time. Differences between the means of control and full-length constructs or siRNA pretreated cells were tested for significance level at $p < 0.05$ using Student's t-test. Confocal imaging and real-time PCR analysis were performed at least three times on different samples.

3. Results

3.1. Differential expression of hRFT -1, -2, and -3 in polarized epithelia

First, we examined the targeting of hRFT-1, hRFT-2, and hRFT-3 in live polarized epithelial cells. Constructs of each full-length riboflavin transporter fused with GFP (GFP-hRFT1, GFP-hRFT2 and GFP-hRFT3) were transiently transfected into intestinal (Caco-2) and renal (MDCK) cells. Live cell confocal imaging was then performed 24–48 hrs following transfection. Lateral (xy) images of cells expressing these constructs showed that these transporters are expressed at the cell surface as well as in intracellular trafficking vesicles in both Caco-2 and MDCK cells (Fig. 1A & C). Axial (xz) images of these cells showed that GFP-hRFT1 was mainly expressed at the BLM of both cell types with some being retained in intracellular vesicular structures (Fig. 1A & C). Expression of GFP-hRFT1 was similar to the known basolaterally localized protein hRFC-GFP (Fig. 1E) [23–25]. In contrast, GFP-hRFT2 was exclusively expressed at the apical membrane domain of both these cell types (Fig. 1A & C; [22]) which mimicked the known apical targeting of hTHTR2-GFP [23, 25] (Fig. 1E). As to hRFT-3, this transporter was found to be localized predominantly within intracellular vesicles, although expression was evident at the BLM of some cells (Fig. 1A & C). Measurement of fluorescence intensities from Caco-2 and MDCK cells showing expression at the respective membrane domains were quantified and confirmed the differential targeting of the hRFT transporters (Fig. 1B & D). We also examined the differential cell surface targeting in single transfected MDCK cell expressing either DsRed-hRFT2/GFP-hRFT1 (Fig. 1F), or DsRed-hRFT2/GFP-hRFT3 (Fig. 1G) to clearly evidence this differential distribution.

As GFP-hRFT3 displayed numerous intracellular trafficking vesicles in many transfected cells, we investigated the characteristics of these structures. Co-transfection of GFP-hRFT1, -2, and -3 with LAMP1-RFP (a late endosomal and lysosomal marker) showed GFP-hRFT1 co-localized with LAMP1-RFP (Fig. 2A) and in contrast, no significant co-localization was found between GFP-hRFT2 and LAMP1-RFP (Fig. 2B) On the other hand, intracellular structures containing GFP-hRFT3 displayed significant co-localization with LAMP1-RFP (Fig. 2C). These results suggests that both basolaterally localized constructs (hRFT-1 and -3) are present on an endosomal population.

3.2. Relative expression of hRFTs mRNA in Caco-2 cells and native human small intestine

To assess the relative amounts of endogenous hRFT-1, -2, and -3 mRNA in well-differentiated Caco-2 cells and native human small intestine, real-time PCR was performed using gene specific primers (Table 1). Results showed the level of the hRFT-2 mRNA was significantly ($p < 0.02$) higher than the level of mRNA for hRFT-1 and -3 in Caco-2 cells (Fig. 3A). Similar observations were also obtained with native human small intestine where expression of hRFT-2 mRNA was significantly higher than that of hRFT-1 ($p < 0.001$) and hRFT-3 ($p < 0.02$) (Fig. 3B).

3.3. Relative functionality of hRFT-1, -2, and -3 in RF uptake

Next, we assessed the ability of hRFT-1, -2, and -3 for transporting RF. For these experiments, an equal amount of cDNA (2 μg/well) encoding hRFT-1, -2, and -3 was transiently transfected into human intestinal epithelial HuTu-80 cells (“Materials and Methods”), followed (48 hrs later) by ^{3}H-RF uptake assays. We chose HuTu-80 cells for these experiments because they are non-polarized yet of intestinal origin, and thus, show no differential membrane expression of these transporters (this was verified by confocal imaging Fig. 4A). Results showed that over-expression of hRFTs in HuTu-80 cells caused a significant induction in carrier-mediated RF uptake ($p < 0.01$ for all) above simultaneously

performed controls. However, the induction caused by hRFT-2 was markedly higher than both hRFT-1 and hRFT-3 ($p < 0.03$, Fig. 4B).

3.4. Contribution of hRFT-2 toward overall carrier-mediated RF uptake by intestinal epithelial cells: gene silencing approach

Having established that hRFT-2 was (i) exclusively expressed at the apical membrane domain, (ii) expressed more abundantly in the human intestine compared to hRFT-1 and -3, and (iii) displayed a greater initial rate of ^{3}H-RF uptake, we next examined the relative contribution of this transporter toward total carrier-mediated RF uptake process across the apical membrane domain. For this we used gene-specific siRNA to knock down hRFT-2 expression in Caco-2 monolayers grown on solid support. Pre-treatment of Caco-2 monolayers with hRFT-2 siRNA caused a significant ($p < 0.01$; ~56%) reduction in the levels of hRFT-2 mRNA expression (Fig. 5A). The reduction only occurred with hRFT-2, mRNA levels of hRFT-1, and -3 actually showed a compensatory increase (86% and 160% for hRFT-1 and -3, respectively). We then examined the effect of the hRFT-2 siRNA treatment on initial-rate of carrier-mediated ^{3}H-RF (0.025 μM) uptake. Data revealed a significant ($p < 0.01$; ~48%) inhibition in ^{3}H-RF uptake in hRFT-2 siRNA-treated compared to scrambled siRNA treated cells (Fig. 5B), despite the compensatory increase in expression of other RF transport isoforms.

4. Discussion

The recent molecular identification of hRFTs has provided a molecular basis for understanding the contributions of each of these individual transporters to the highly efficient and specific process of intestinal RF uptake. Here we show unique targeting of each family member in polarized cells: hRFT-1 is expressed basolaterally, hRFT-2 is expressed apically [22] and hRFT-3 is distributed between an endosomal reservoir and the basolateral cell surface. Resolution of this polarized expression of hRFT family members defines the likely molecular identity of the systems involved in carrier-mediated RF transport across the apical (hRFT-2) and basolateral (hRFT-1) membrane domains that have been previously observed in radioligand uptake experiments [15–18]. The apical localization of hRFT-2 and the differential targeting of hRFT-1 basolaterally are immediately suggestive of a route for vectorial transport of RF from the intestinal lumen to the bloodstream that is achieved by differential targeting of discrete transporter isoforms. The existence of a third family member (hRFT-3) likely provides further customizability for regulation of RF homeostasis and trans-epithelial transport. The intracellular localization of this transporter within a population of structures co-expressing LAMP-1 is perhaps suggestive of an adaptively regulated transporter pool that can undergo regulated translocation to/from the BLM. Further experiments, however, are needed to assess this possibility.

Quantification of endogenous levels of hRFTs mRNAs revealed higher levels of hRFT-2 compared with hRFT-1 and hRFT-3 in both native human intestine and Caco-2 cells. This finding confirms an earlier observation on the expression of RFTs in native human intestine [19]. Further, both gain of function and loss of function analyses highlighted a dominant contribution of hRFT-2 to cellular ^{3}H-RF uptake. Specifically, overexpression of hRFT-2 increased the initial rate of ^{3}H-RF uptake to a greater extent than the two other hRFTs. Knockdown of hRFT-2 resulted in a significant (~48%) decreased ^{3}H-RF uptake despite compensatory increases in expression of hRFT-1 and hRFT-3. Such findings when considered in conjunction with observations that the kinetic parameters of RF uptake process by Caco-2 cells are similar to those displayed by hRFT-2 [28], and that RF deficiency leads to an induction in intestinal RF uptake [28] and in RFT-2 expression (but not RFT-1, [29] unpublished observations from our laboratory), make it reasonable to conclude that hRFT-2 plays a predominant role in intestinal RF absorption process.

In summary, hRFT-2 is expressed at the apical membrane domain and functions to facilitate RF entry into absorptive epithelia. Expression of hRFT-1 and to some extent hRFT-3, at the BLM suggests these systems are responsible for regulating RF exit out of absorptive epithelia (and possibly for RF uptake from blood in the absence of luminal RF).

Acknowledgments

This study was supported by grants from the Department of Veterans Affairs and the National Institutes of Health (DK84094 to VSS, GM088790 to JSM and DK56061 and DK58057 to HMS).

List of abbreviations

LAMP1 lysosome associated membrane protein1

References

1. Cooperman, JM.; Lopez, R. Riboflavin. In: Machlin, LJ., editor. Handbook of vitamins: Nutritional, Biochemical and Clinical Aspects. New York: Dekker; 1984. p. 299-327.
2. Fernandez-Banares F, Abad-Lacruz A, Xiol X, Gine JJ, Dolz C, Cabre E, Esteve M, Gonzalez-Huix F, Gassull MA. Vitamin status in patients with inflammatory bowel disease. Am J Gastroenterol. 1989; 84:744–748. [PubMed: 2500847]
3. Dreizen S, McCredie KB, Keating MJ, Andersson BS. Nutritional deficiencies in patients receiving cancer chemotherapy. Postgrad Med. 1990; 87:163, 167–170. [PubMed: 2296564]
4. Kodentsova VM, Vrzhesinskaia OA, Sokol'nikov AA, Kharitonchik LA, Spirichev VB. Metabolism of B group vitamins in patients with insulin-dependent and non-insulin dependent forms of diabetes mellitus. Vopr Med Khim. 1993; 39:26–29. [PubMed: 8279137]
5. Bonjour JP. Vitamins and alcoholism. V. Riboflavin, VI. Niacin, VII. Pantothenic acid, and VIII. Biotin. Int J Vitam Nutr Res. 1980; 50:425–440. [PubMed: 7009467]
6. Rosenthal WS, Adham NF, Lopez R, Cooperman JM. Riboflavin deficiency in complicated chronic alcoholism. Am J Clin Nutr. 1973; 26:858–860. [PubMed: 4541718]
7. Glodsmith, GA. Riboflavin deficiency. In: Rivlin, R., editor. Riboflavin. New York: Plenum; 1975. p. 221-224.
8. Pangrekar J, Krishnaswamy K, Jagadeesan V. Effects of riboflavin deficiency and riboflavin administration on carcinogen-DNA binding. Food Chem Toxicol. 1993; 31:745–750. [PubMed: 8225133]
9. Wrong, OM.; Edmonds, CJ.; Chadwich, VS. wiley and Sons. In The Large Intestine; Its Role In mammalian Nutrition and Homeostasis. New York: 1981. Vitamins; p. 157-166.
10. Said HM, Ortiz A, Moyer MP, Yanagawa N. Riboflavin uptake by human-derived colonic epithelial NCM460 cells. Am J Physiol Cell Physiol. 2000; 278:C270–276. [PubMed: 10666022]
11. Iinuma S. Synthesis of riboflavin by intestinal bacteria. J Vitaminol (Kyoto). 1955; 1:6–13. [PubMed: 13264325]
12. Kasper H. Vitamin absorption in the colon. Am J Proctol. 1970; 21:341–345. [PubMed: 5483294]
13. Olcese O, Pearson PB, Schweigert BS. The synthesis of certain B vitamins by the rabbit. J Nutr. 1948; 35:577–590. [PubMed: 18914203]
14. Said HM. Recent advances in carrier-mediated intestinal absorption of water-soluble vitamins. Annu Rev Physiol. 2004; 66:419–446. [PubMed: 14977409]
15. Said HM, Arianas P. Transport of riboflavin in human intestinal brush border membrane vesicles. Gastroenterology. 1991; 100:82–88. [PubMed: 1983852]
16. Said HM, Hollander D, Mohammadkhani R. Uptake of riboflavin by intestinal basolateral membrane vesicles: a specialized carrier-mediated process. Biochim Biophys Acta. 1993; 1148:263–268. [PubMed: 8504119]

17. Said HM, Mohammadkhani R. Uptake of riboflavin across the brush border membrane of rat intestine: regulation by dietary vitamin levels. Gastroenterology. 1993; 105:1294–1298. [PubMed: 8224633]
18. Said HM, Mohammadkhani R, McCloud E. Mechanism of transport of riboflavin in rabbit intestinal brush border membrane vesicles. Proc Soc Exp Biol Med. 1993; 202:428–434. [PubMed: 8456106]
19. Yao Y, Yonezawa A, Yoshimatsu H, Masuda S, Katsura T, Inui K. Identification and comparative functional characterization of a new human riboflavin transporter hRFT3 expressed in the brain. J Nutr. 2010; 140:1220–1226. [PubMed: 20463145]
20. Yonezawa A, Masuda S, Katsura T, Inui K. Identification and functional characterization of a novel human and rat riboflavin transporter, RFT1. Am J Physiol Cell Physiol. 2008; 295:C632–641. [PubMed: 18632736]
21. Yamamoto S, Inoue K, Ohta KY, Fukatsu R, Maeda JY, Yoshida Y, Yuasa H. Identification and functional characterization of rat riboflavin transporter 2. J Biochem. 2009; 145:437–443. [PubMed: 19122205]
22. Subramanian VS, Rapp L, Marchant JS, Said HM. Role of cysteine residues in cell surface expression of the human riboflavin transporter-2 (hRFT2) in intestinal epithelial cells. Am J Physiol Gastrointest Liver Physiol. 2011
23. Subramanian VS, Marchant JS, Said HM. Targeting and trafficking of the human thiamine transporter-2 in epithelial cells. J Biol Chem. 2006; 281:5233–5245. [PubMed: 16371350]
24. Subramanian VS, Marchant JS, Said HM. Apical membrane targeting and trafficking of the human proton-coupled transporter in polarized epithelia. Am J Physiol Cell Physiol. 2008; 294:C233–240. [PubMed: 18003745]
25. Boulware MJ, Subramanian VS, Said HM, Marchant JS. Polarized expression of members of the solute carrier SLC19A gene family of water-soluble multivitamin transporters: implications for physiological function. Biochem J. 2003; 376:43–48. [PubMed: 14602044]
26. Subramanian VS, Subramanya SB, Tsukamoto H, Said HM. Effect of chronic alcohol feeding on physiological and molecular parameters of renal thiamin transport. Am J Physiol Renal Physiol. 2010; 299:F28–34. [PubMed: 20427470]
27. Livak KJ, Schmittgen TD. Analysis of relative gene expression data using real-time quantitative PCR and the 2(−Delta Delta C(T)) Method. Methods. 2001; 25:402–408. [PubMed: 11846609]
28. Said HM, Ma TY. Mechanism of riboflavine uptake by Caco-2 human intestinal epithelial cells. Am J Physiol. 1994; 266:G15–21. [PubMed: 8304455]
29. Fujimura M, Yamamoto S, Murata T, Yasujima T, Inoue K, Ohta KY, Yuasa H. Functional characteristics of the human ortholog of riboflavin transporter 2 and riboflavin-responsive expression of its rat ortholog in the small intestine indicate its involvement in riboflavin absorption. J Nutr. 2010; 140:1722–1727. [PubMed: 20724488]

Highlights

- This study provides evidence for the importance of hRFT-2 in normal intestinal riboflavin absorption.
- The study also identifies which membrane domain of polarized epithelia the hRFT-1, -2 and -3 transporters are expressed.
- hRFT-2 is the most active and predominantly expressed RFT in normal intestine.

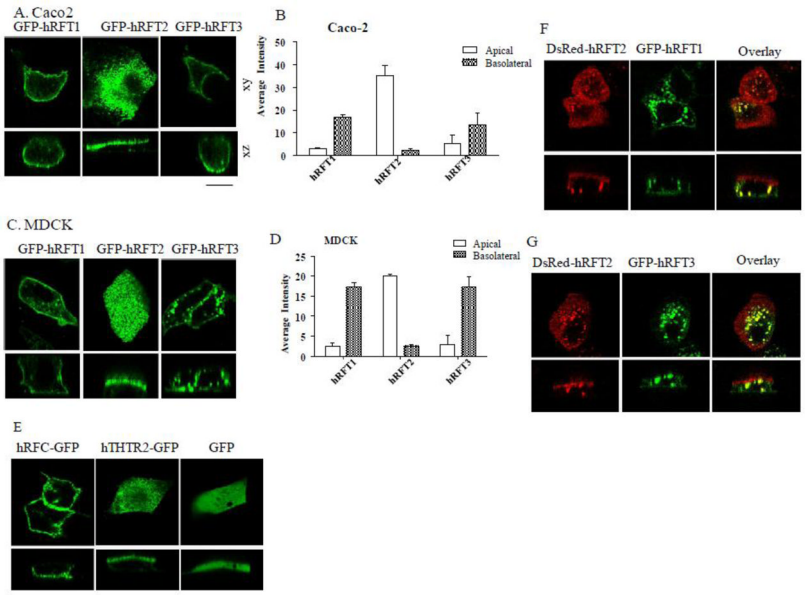

Fig. 1. Polarized membrane localization of GFP-hRFT-1, -2, and -3 in Caco-2 and MDCK cells

A & C) Lateral (xy) and axial (xz) sections of Caco-2 and MDCK cells, expression for indicated constructs. B & D) Average fluorescence intensity at indicated membrane domains for all indicated transporters in Caco-2 and MDCK cells (n ≥10 cells)[25]. E) hRFC-GFP, hTHTR2-GFP and GFP expressing MDCK cells; note the cytosolic expression of GFP alone. F & G) Lateral (xy) and axial (xz) confocal sections of MDCK cells transiently co-expressed with DsRed-hRFT2 and GFP-hRFT1 or DsRed-hRFT2 and GFP-hRFT3 as indicated. Scale bar 10μm. Representative images from at least three independent experiments were shown for indicated constructs.

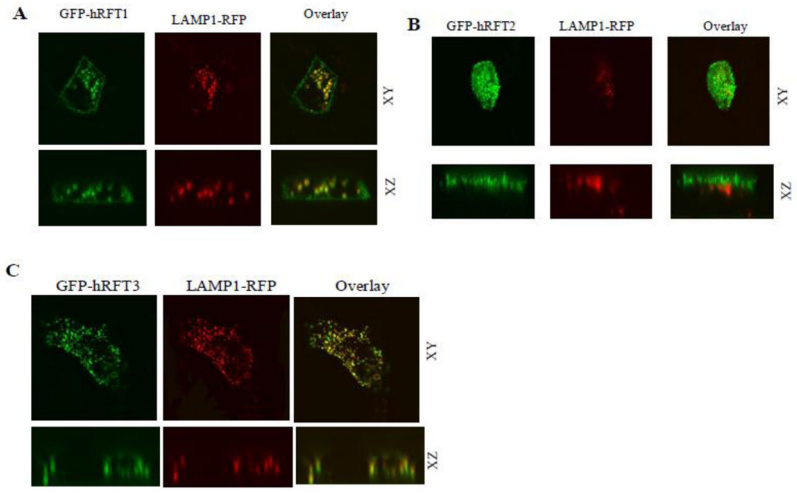

Fig. 2. Subcellular co-localization of GFP-hRFT1, -2, or -3 with LAMP1-RFP in MDCK cells

MDCK cells were transiently co-transfected with GFP-hRFT1, -2, or -3 and LAMP1-RFP. Representative images from at least three separate experiments were shown for indicated constructs.

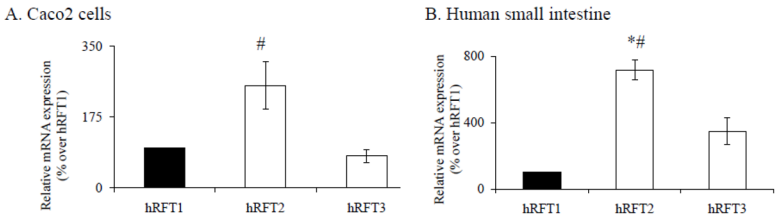

Fig. 3. Relative expression of hRFTs mRNA levels in Caco-2 and in native human small intestine

Quantitative real-time RT-PCR was performed on RNA isolated from Caco-2 cells (A) and native human small intestine (B) using hRFT-1, -2, and -3 gene specific primers as described in "Materials and Methods". Data are mean ± SE of at least three independent experiments performed in different occasions. * $p < 0.001$, # $p < 0.02$.

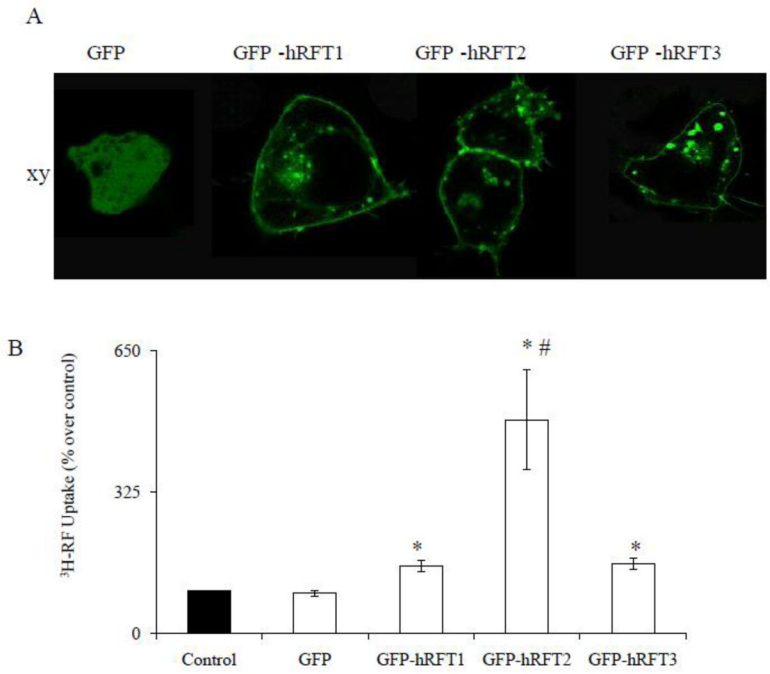

Fig. 4. Efficiency of hRFTs in transporting RF

A) Lateral (xy) sections of confocal images of GFP-hRFT1, -2, -3 and GFP alone expressing HuTu-80 cells B) GFP, GFP-hRFT1, -2, and -3 transiently expressing HuTu-80 cells were incubated in Kreb's-Ringer buffer (pH 7.4) containing ^{3}H-RF (0.025 μM) for 3 min at 37°C. Data are mean ± SE of at least three uptake determinations performed in three different occasions. * $p < 0.01$ and # $p < 0.03$.

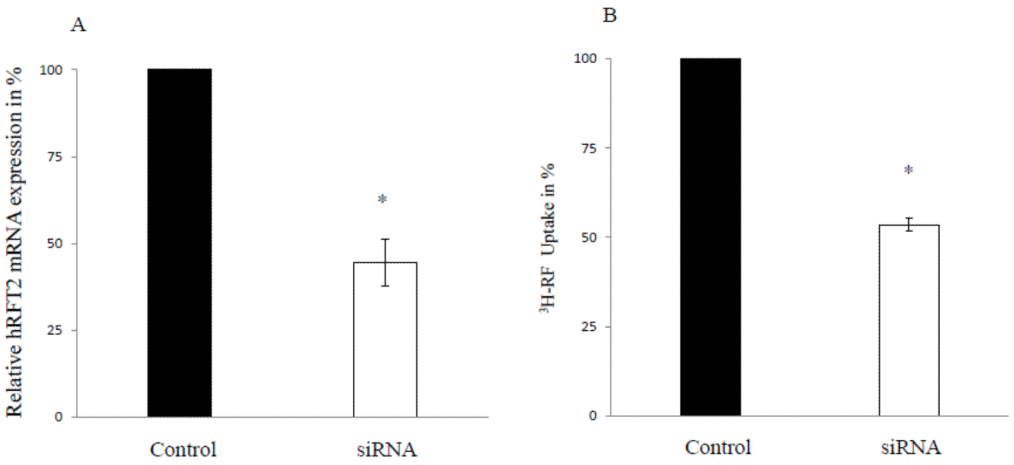

Fig. 5. Effect of gene-specific hRFT-2 siRNA on the level of expression of hRFT2 and RF uptake

A) Real-time RT-PCR was performed as described above on total RNA isolated from control (scrambled) and hRFT-2 gene-specific siRNA pretreated Caco-2 cells. B) Uptake was performed in control and hRFT-2 siRNA pretreated Caco-2 cells as described in Figure legend 4. Data are mean ± SE of at least three separate uptake and PCR determinations performed in three different occasions. * $p < 0.01$.

Table 1

Combination of PCR primers used to prepare the full-length hRFT-1,-2 and -3 constructs of by PCR

Construct	Forward & Reverse Primers (5′-3′)	Positions (bp)	Fragment (bp)
GFP-hRFT1[1–448]	CCC***AAGCTT***ATGGCAGCACCCACGCT; TCC**CCGCGG**GGGGCCACAGGGGTCTAC	1–1344	1344
GFP-hRFT2[1–469]	CCG*CTCGAG*ATGGCCTTCCTGATGCAC; CGGGATCCGGCTGGACAGTGCAGATTGCA	1–1407	1407
DsRed-hRFT2[1–469]	GC**GTCGAC**ATGGCCTTCCTGATGCAC; CGGGATCCGGCTGGACAGTGCAGATTGCA	1–1407	1407
GFP-hRFT3[1–455]	CCC***AAGCTT***ATGGCAGCACCCACGCCCGCC; TCC**CCGCGG**GGAGTCACAGGGGTCTGCACA	1–1365	1365
Real-time PCR primers			
hRFT-1	AAAAGACCTTCCAGAGGGTTG; AGCACCTGTACCACCTGGAT		
hRFT-2	CCTTTCCGAAGTGCCCATC; AGAAGGTGGTGAGGTAGTAGG		
hRFT-3	CCCTGGTCCAGACCCTA; ACACCCATGGCCAGGA		
β-actin	AGCCAGACCGTCTCCTTGTA; TAGAGAGGGCCCACCACAC		
hRFT-2 si RNA sequence			
CCG GCG CAC CUG UUC AUC UAU A; UCC UGC CUA ACA GGU CUC UGC UGU U			

Table 1 shows the primer sequences and combinations used to generate each construct.

Restriction sites *Hind III* (bold face italics text) and *Sac II* (boldface underlined text) for hRFT-1 and -3 and *XhoI* (boldface text)/*Sal I* (italics), and *Bam HI* (underlined text) for hRFT-2 were added to the primers to allow subsequent sub-cloning into the GFP-C3 or DsRed-C1vectors.